

# Ultraviolet Radiant Energy From the Sun Observed At 11,190 Feet

Ralph Stair

This paper gives the results of some measurements on the ultraviolet and short wavelength visible spectral energy distribution of direct solar radiation, made in September 1951, at Climax, Colo., altitude 11,190 feet. Data are given for wavelengths extending from 535 to 299.5 millimicrons for a number of air masses from 0 to 3.0). A determination of atmospheric transmittance as a function of wavelength results in calculated amounts of ozone approximating 0.21 centimeter (*ntp*) for several days during September. This value is in good agreement with previous determinations by other methods, for the season of the year and the geographical latitude of Climax.

## 1. Introduction

A preliminary determination of the distribution of radiant energy in the ultraviolet solar spectrum made at Washington, D. C., in 1950 was previously reported [1, 2].<sup>1</sup> This work, having shown great promise for the instruments and method employed, induced the attempt to make similar measurements at a high-altitude station. An invitation from Donald H. Menzel to make use of one of the Harvard high-altitude stations for this work was opportune. After a survey of the expected weather conditions and the available accommodations at possible high-altitude locations, the Climax, Colo. station was chosen for the month of September 1951.

Climax, Colo. is located on the continental divide in the heart of the Rocky Mountains about 100 miles southwest of Denver. A location at the new observatory station on Chalk Mountain, about 2½ miles west of Climax, was assigned for the work. At this point the altitude is approximately 11,190 ft, so that about 35 percent, by pressure, of the atmosphere is below the observer. The longitude and latitude of the station are approximately 106° 12'30" W and 39°23'45" N, respectively. Climax was originally chosen by the scientific personnel of Harvard University and the University of Colorado for use as a high-altitude observatory for the study of solar radiation because of its exceptional climatic conditions.

At the temperatures prevailing within the solar body, the atoms are multiply ionized. Only in the outer layers of the solar atmosphere, where lower temperatures prevail, do neutral and singly ionized atoms occur and also small quantities of a few diatomic molecules (for example, NH, OH, CN, etc.). Solar-absorption—Fraunhofer lines—results, therefore, primarily from absorption by hydrogen and by neutral and singly ionized atoms of iron, calcium, aluminum, titanium, chromium, magnesium, and other elements in the solar atmosphere.

According to current concepts of nuclear physics [3], the solar energy is produced through the transformation of hydrogen into helium within the highly

heated central nucleus of the sun. The resulting gamma rays are absorbed by the overlying gas layers, which gradually transmit the generated energy to the solar surface. In general, it probably requires thousands of years by this process for a specific bundle of energy to reach the radiating layer, during which time its wavelength distribution has been reduced to that approximating a black body near 6,000° K. At times flares are ejected at terrific velocities from lower solar levels of very high temperature resulting not only in marked changes in the radiating surface but in increased emission by the flares themselves. According to Dodson [18], the emission in these flares is primarily due to atomic hydrogen. In the course of continuous observations during a time of excessive solar activity as many as 83 flares, for which the H<sub>α</sub> intensity was estimated to be at least four times the solar background, have been observed within a period of 105 hr [19].

The amount and the spectral quality of the solar radiant energy reaching the earth's surface is also affected by absorption of energy by certain vapors, gases, or dust within the terrestrial atmosphere. One of these, ozone, was suspected [4], at an early stage in astrophysics, because of the fact that the spectra of all the stars, including the sun, terminated at about 300 mμ.

The total solar radiant energy varies slightly from time to time. Furthermore, it can be shown from Planck's law that the variations are more pronounced in the ultraviolet spectrum. But another factor enters the picture; namely, with greater short-wavelength intensity more ozone will be produced in the upper atmosphere. This results in a lower atmospheric transmittance within the spectral region of 300 to 330 mμ. Hence, although more ultraviolet may be emitted, the amount passing through our atmosphere may change but little or actually be less than normal.

## 2. Instruments and Procedure

The observations on the spectral distribution of the radiant energy from the sun at Climax, Colo., were made with the same Farrand double quartz-

<sup>1</sup> Figures in brackets indicate the literature references at the end of this paper.

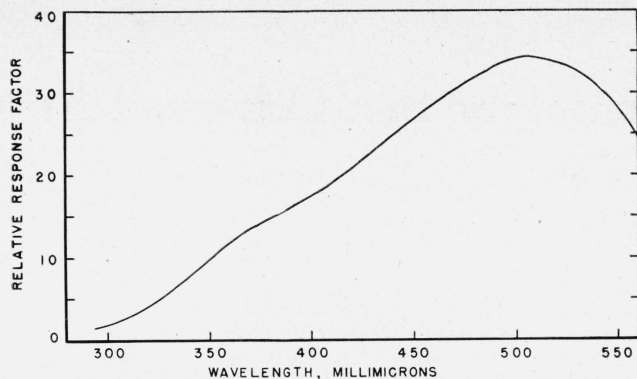


FIGURE 1. *Relative spectral-response factors for the complete spectroradiometer as employed in the Climax measurements.*

935 phototube, slit setting=0.09 mm.

prism spectrometer and auxiliary equipment (consisting of the RCA type 935 phototube, 510-cycle light modulator, tuned amplifier, Ballantine a-c vacuum-tube voltmeter, and Leeds & Northrup type A Speedomax recorder) as previously employed at Washington [1, 2], except that a new type of siderostat (designed to follow the sun) developed by the Optical Division of the Naval Research Laboratory was employed to reflect the sunlight into the spectroradiometer.

The entire equipment, except for the siderostat, was set up in a quonset hut with the entrance slit of the spectrometer toward the south. Through a small opening in one of the windows of the building a beam of sunlight was reflected through the entrance slit of the spectrometer onto the center of the first lithium-fluoride-quartz collimating lens of the instrument.

The siderostat was of simple design, arranged so that a primary (plane aluminized) mirror reflected the beam of light along the polar axis of the instrument. A second stationary mirror reflected the beam horizontally into the spectrometer. Thus each of the mirrors operated at fixed angles relative to the light beam during the day. A synchronous motor-drive provided for the automatic following of the sun during the course of each day's observations.

To assist in the proper alinement of the siderostat and spectrometer and to reduce the amount of sky radiation entering the spectroradiometer to a very low value, diaphragms equivalent to about 2- by 4-in. openings were placed at approximately 2 ft and 5 ft from the entrance slit of the spectrometer. These, together with the relatively extensive distance (about 8 ft) between the primary siderostat mirror (approximately 2 by 4 in.) and the spectroradiometer aided in keeping the solar beam on the optical axis of the instrument.

In accordance with the procedure in the previous work [1], no lens or mirror was employed to produce an image of the sun on the entrance slit of the spectrometer because an integrated solar energy spectrum was desired. Although the spectroradiometer

was not used most efficiently, according to general optical principles, because only a small part of the total available aperture was employed, it was expedient to operate in this manner to eliminate variations in light transmittance through partial cut-off at the edges of some of the optical parts.

The accurate adjustment and calibration of the wavelength scale of the instrument was accomplished through the use of a mercury-arc discharge lamp. After being unpacked and installed, each section of the spectrometer was individually adjusted for highest energy transmittance, and the combination was locked-in for best adjustment at the 313.2 and 405-m $\mu$  emission lines. Wavelength settings of the instrument were recorded for each of the intense mercury emission lines between 313.2 and 578 m $\mu$  for application to the recorded data on the sun and on a tungsten-filament-in-quartz lamp, which was employed in the radiant energy evaluations. The Fraunhofer lines lend themselves ideally for use as wavelength standards in the measurement of solar spectral radiant energy. However, no such indices are present in the spectrum of the tungsten-filament-in-quartz lamp, so that a precise wavelength calibration, together with a system of chart index marking was highly advantageous. For this purpose, an index pen on the upper part of the recorder chart provided an automatic method of wavelength identification on the chart records. Index marks at regular intervals defined specific wavelengths, so that the three sets of data, that for the mercury arc, the tungsten-filament-in-quartz lamp, and that for the sun, were readily compared for wavelength and relative spectral intensity.

The tungsten-filament-in-quartz lamp, manufactured by the Westinghouse Electric Corporation and described in detail elsewhere [2, 7] was employed in the spectral radiant energy calibration of the entire spectroradiometer, including all the optical and electronic parts from the first siderostat mirror to the recorder. The lamp served both as a standard for relative spectral intensity and for absolute intensity, in microwatts per square centimeter per unit wavelength. This lamp was standardized in terms of color temperature [8], and its spectral radiant energy was evaluated through the application of published spectral emissivity data on tungsten [9 to 12]. The true temperature of 2,805° K, characteristic of the radiation from the lamp, determined on the basis of the observed color temperature and the emissivity values of tungsten, establishes the spectral radiant energy distribution for the lamp.

The reduction of the data on the spectral distribution of the ultraviolet radiant energy from the sun was accomplished in a manner similar to that previously reported [1, 2]. Most of the essential data employed in this evaluation are given in table 1, illustrating the various steps involved in obtaining the instrumental spectral response factors (see fig. 1).

In the present work the entrance and middle slits of the spectrometer were set at about 0.09 mm—a value that gave a resolution of about 1 m $\mu$  at 300 m $\mu$  (to 2 to 3 m $\mu$  at longer wavelengths). The final

TABLE 1. *Relative spectral-energy data on standard tungsten-filament-in-quartz lamp and its application in the calibration of the spectral-response factor of the spectroradiometer*

Wave length	Relative energy black body $T=2805^{\circ}\text{K}$ $C_2=14,380$	Emissivity of tungsten	Relative spectral energy from lamp	Absolute energy from lamp in $(\mu\text{w}/\text{cm}^2)/\text{m}\mu$ at 1 meter	Recorder response reduced to amplifier sensitivity 1	Instrumental spectral response factors (col. 6÷5)
1	2	3	4	5	6	7
$m\mu$						
300	66.2	0.422	27.9	0.048	0.00087	0.0181
310	97.4	.427	41.6	.072	.00215	.0299
320	139	.433	60.2	.104	.0043	.0413
330	195	.438	85.4	.148	.0087	.0588
340	264	.443	117.0	.202	.0155	.0767
350	351	.447	156.9	.271	.0268	.0989
360	459	.448	205.6	.356	.0429	.1205
370	588	.450	264.6	.457	.0613	.1341
380	741	.451	334.2	.577	.0849	.1471
390	920	.452	415.8	.719	.1150	.1599
400	1126	.452	509.0	.880	.153	.1739
410	1361	.453	616.5	1.066	.203	.1904
420	1624	.452	734.0	1.269	.264	.2080
430	1917	.451	864.6	1.495	.343	.2294
440	2241	.449	1006.2	1.740	.435	.2500
450	2595	.448	1162.6	2.010	.543	.2701
460	2978	.447	1331	2.302	.663	.2880
470	3381	.445	1505	2.603	.791	.3039
480	3830	.444	1701	2.942	.937	.3185
490	4296	.442	1899	3.283	1.083	.3299
500	4787	.441	2111	3.651	1.233	.3377
510	5301	.441	2338	4.043	1.380	.3413
520	5837	.440	2568	4.440	1.495	.3367
530	6392	.440	2812	4.863	1.584	.3257
540	6964	.439	3057	5.286	1.626	.3076

slit was then set at the minimum value such that most of the radiant energy passing through the first two slits reached the phototube at all wavelength settings between 300 and 600  $m\mu$ .

For operation of the equipment, commercial 110-v., 60-cycle alternating current was available. Frequency control was assured through interpower connections, but voltage fluctuations were very large, probably partly because of heavy and irregular power consumption at the nearby plant of the Climax Molybdenum Co. The voltage changes, however, usually remained within the control limits of a 1,000-v-a voltage regulator that had been incorporated into the equipment. It was only during a single temporary power failure that measurements were interrupted because of power difficulties.

Measurements of the spectral radiant energy from the sun were made at Climax over a period of about 3 weeks during September 1951. On each day, except when clouds interfered, data were taken between about 7.30 a. m. and 4.30 p. m. Trees and mountains prevented observations at earlier or later hours. These limitations, together with the season of the year, confined the measurements to solar angles (zenith distances) corresponding to air masses between about 1.25 and 3.00.<sup>2</sup> Snow and the accompanying cloudiness interrupted the work on several days. During the 3 weeks (September 6 to 27) there were three snowfalls, totaling approximately 7 in. These not only rendered the air more free of haze and smoke but kept down much dust occasioned by temporary public and private road

<sup>2</sup> "Air mass" as employed here refers to the amount of atmosphere traversed by the solar rays. It is numerically equal to the secant of the zenith angle of the sun.

construction and by heavy traffic over nearby unpaved roads.

Usually the data were recorded in the general order illustrated in figure 2, except that each curve was

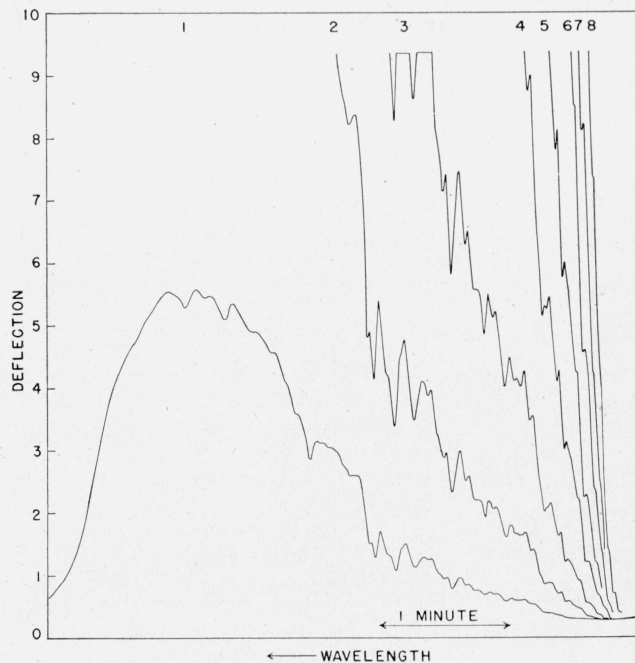


FIGURE 2. *Representative data taken from a section of the recorder chart.*

September 26, 1951, approximately 10:30 a. m., air mass 1.40.

repeated before passing on to the next amplifier setting. Ordinarily the amplifier was first set at a high sensitivity (sensitivity 8) so that only the spectral intensities for the shorter wavelengths appeared on the chart. Successively lower amplifier sensitivity settings (7 to 1) were made so that different parts of the solar spectrum appeared on the upper portion of the chart, the previously recorded values being compressed on the lower part of the record. Usually the small interval of time (about 1 to 2 min.) between records reflected the change in solar intensity resulting from the small change in the sun's zenith distance, or in the air mass. An appreciable range of the solar ultraviolet spectrum was thus automatically plotted within a very short interval of time. This rapid scanning speed, made possible by the high sensitivity of the detecting and amplifying equipment, was many times faster than that obtainable through the photographic or the point-by-point radiometric methods previously employed by other observers [4, 21, 25].

Except for a few days during the early part of the work, the temperature within the building surrounding the spectroradiometer and recording equipment was maintained at 70° F (plus or minus a few degrees). Ordinarily the electronic equipment was placed in operation about 30 min or more before data were recorded and was left in continuous operation until measurements were concluded for the day. As a further check on the sensitivity of the electronic equipment throughout each day, numerous checks were made through the use of a secondary standard lamp that could be momentarily placed in front of the spectrometer entrance slit.

Since in a lens-prism spectrometer there are a number of reflecting surfaces (on the lenses and prism faces) where the transmitted beam is incident at angles differing from the normal, a certain amount of polarization of the transmitted energy necessarily

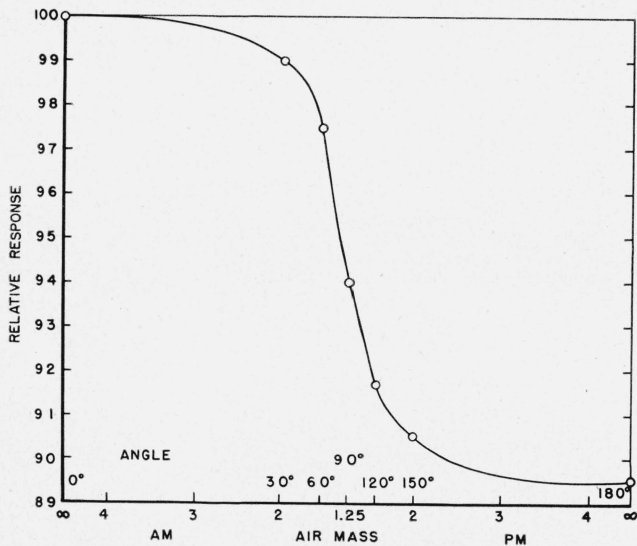


FIGURE 3. Relative response of the complete equipment as affected by light polarization by the siderostat and the spectrometer.

Polarization factor versus air mass.

occurs. Furthermore, since there are two mirror reflections of the light beam by the siderostat before it enters the spectroradiometer, there is a varying amount and direction of polarization in the incident beam. As a result of the combined polarizations, the amount of radiant energy reaching the phototube varies as some function of the relative angles of the optical elements of the system. In the case of all the optical components, except the primary siderostat mirror, there was little change in the angle orientations during the measurements at Climax. A study was made therefore to determine the amount by which the transmitted radiant energy was affected by the combined polarization effects of the siderostat and spectroradiometer as functions of both the wavelength and the primary mirror angle. The results of this investigation indicated that for wavelengths shorter than about 550m $\mu$  the polarization effects were independent of wavelength of incident radiation within 1 percent. An over-all change approximating 10 percent in the transmitted energy occurred between an angular setting of 30° and 150°, that is, between positions of the sun corresponding to air mass 2.0 in the morning and air mass 2.0 in the afternoon. These data are summarized by the curve in figure 3.

### 3. Spectral Solar Energy Curve

The observations of the solar spectral energy distribution requires measurements on a source that is rapidly changing in intensity and spectral quality. The small (sometimes large) fluctuations resulting from variations in the transmission characteristics of the terrestrial atmosphere are largely eliminated through making the measurements at a high-altitude station above most of the dust and smoke commonly present in the lower terrestrial atmosphere.

Data on the spectral solar radiant energy are given in table 2 for a single solar zenith angle corresponding to air mass (secant  $Z$ )=1.40 for four of the days during which extensive series of measurements were made. Mean values for a number of selected air masses are given in table 3. Data on other days during the investigation, and not included in these tables, differ but little from those employed in the preparation of the tables. Data for selected air masses fall approximately on a straight line (see fig. 4) when plotted in terms of the logarithm of the deflection (intensity) as a function of air mass. Extrapolating these lines to air mass 0 gives the logarithms of numbers representing the spectral solar intensity outside the earth's atmosphere. From determinations at about 25 separate wavelengths between 300 and 540 m $\mu$  for each of the 4 days (approximately 100 determinations) the  $M_0$  factor in column 7 of table 2 was determined from a smooth curve passing through a plot of the wavelength against the multiplying factors required to give the values of the intercepts at air mass 0. Most of the data for one day (September 26) employed in this evaluation are shown in figure 4. The slopes of these lines define the atmospheric transmission coefficients discussed in greater detail below.

TABLE 2. Spectral distribution of radiant energy from the sun, Climax, Colo., September 1951

Altitude of station, 11,190 ft. Air mass 1.40 and outside the atmosphere, air mass 0.  
Energy in microwatts per square centimeter per 10 mμ.

1	2	3	4	5	6	7	8
Wavelength	Sept. 16. Air mass 1.40	Sept. 17. Air mass 1.40	Sept. 19. Air mass 1.40	Sept. 26. Air mass 1.40	Mean. Air mass 1.40	M <sub>0</sub> factor	I <sub>0</sub> Air mass 0
mμ							
299.5	7.1	6.1	6.3	7.2	6.7	100	670
302.5	9.3	14.0	14.7	15.0	13.3	55.7	741
304	46.9	40.9	43.0	41.7	43.1	28.9	1246
306	72.3	65.2	71.1	73.1	70.4	16.7	1176
309.2	128.3	120.1	124.5	130.4	125.8	10.2	1283
310	124.7	114.6	120.0	126.7	121.5	8.60	1045
312	223	208	215	222	217.0	6.38	1384
314.9	267	255	261	269	263.0	5.05	1328
315.8	280	267	275	283	276	4.64	1282
316.5	269	247	256	266	260	4.30	1116
317.9	378	350	360	375	366	3.87	1415
318.5	353	325	338	350	342	3.85	1315
321.1	435	408	413	429	421	3.48	1466
321.7	418	389	396	410	404	3.40	1372
322.8	404	380	384	397	391	3.25	1272
323.5	388	360	366	377	373	3.15	1174
325.5	469	422	451	461	451	2.97	1339
327.5	622	567	581	592	591	2.78	1642
328.5	589	542	553	565	562	2.69	1512
330.3	682	645	659	667	663	2.57	1705
331.5	610	578	587	602	594	2.50	1486
332.9	614	575	591	606	597	2.45	1461
333.6	603	566	580	592	585	2.42	1416
335.3	619	593	596	609	604	2.36	1426
337	542	510	526	526	526	2.30	1210
337.5							
340.8	652	615	638	634	635	2.33	1415
341.7	626	589	614	605	609	2.21	1345
343.5	642	604	628	621	624	2.18	1360
345	540	505	527	523	524	2.15	1126
348.6	586	550	569	613	580	2.09	1211
351.5	636	601	619	606	616	2.04	1256
352.6	593	565	584	574	579	2.02	1170
355.1	684	646	669	648	662	1.97	1304
358	500	470	486	484	485	1.92	931
360	620	594	625	625	616	1.89	1164
361	604	567	581	595	587	1.87	1097
363.8	676	626	638	660	650	1.84	1196
367.1	806	772	799	818	799	1.80	1438
368.6	773	744	773	770	765	1.79	1369
371	803	774	801	795	793	1.76	1396
375	649	623	645	645	641	1.72	1101
379.4	870	846	873	871	865	1.69	1462
380.7	815	799	828	820	816	1.68	1370
385	575	554	573	574	569	1.66	945
387.7	710	694	710	706	705	1.64	1156
391.5	891	874	894	898	889	1.62	1441
394	665	633	659	657	654	1.60	1046
396.1	778	740	768	776	766	1.58	1209
397.0	759	716	748	757	745	1.57	1170
403.3	1355	1254	1294	1276	1295	1.52	1968
406	1301	1202	1244	1240	1247	1.50	1870
410	1333	1228	1290	1310	1290	1.47	1897
416.8	1410	1331	1362	1355	1365	1.43	1951
421	1396	1315	1348	1343	1351	1.40	1891
424	1362	1297	1320	1325	1326	1.38	1830
428	1197	1137	1156	1159	1162	1.35	1569
432	1363	1306	1322	1348	1335	1.34	1789
436	1408	1346	1361	1374	1372	1.33	1825
441	1552	1513	1505	1540	1528	1.31	2001
447	1647	1591	1594	1617	1613	1.29	2080
455.7	1672	1630	1630	1641	1643	1.28	2103
468	1561	1518	1522	1535	1534	1.26	1933
482	1612	1571	1569	1577	1582	1.25	1978
487	1501	1473	1463	1473	1478	1.24	1832
497	1566	1547	1532	1547	1548	1.23	1904
500	1549	1527	1516	1533	1531	1.22	1868
509	1578	1558	1545	1555	1559	1.21	1886
520	1518	1491	1481	1491	1495	1.20	1794
526	1612	1573	1569	1579	1583	1.195	1892
530	1643	1621	1598	1618	1620	1.19	1928
535	1583	1566	1541	1591	1570	1.185	1861

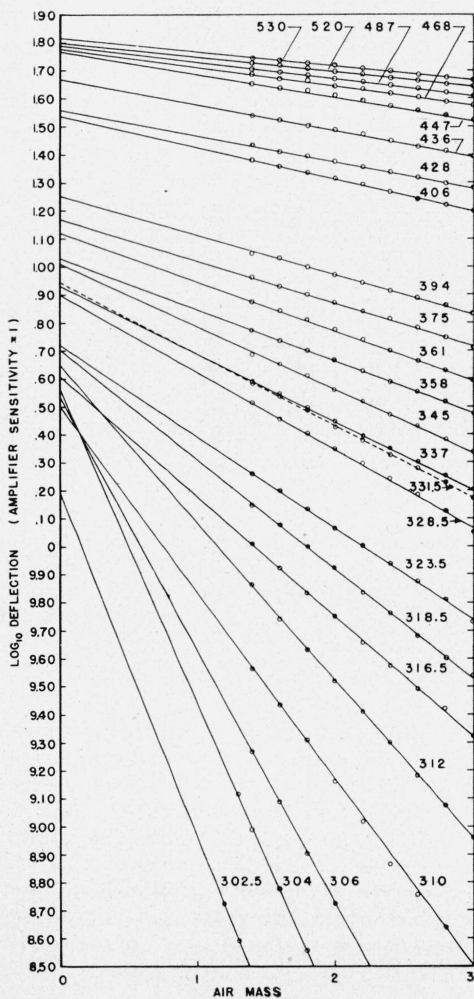


FIGURE 4. Determination of the solar intensity outside the atmosphere through graphing the logarithm of the observed data as a function of the solar angle (air mass).  
Climax, Colo., September 26, 1951.

TABLE 3. Spectral distribution of radiant energy from the sun for selected air masses, Climax, Colo.

Altitude 11,190 ft. Mean for 4 days in September 1951. Radiant energy in microwatts per square centimeter per 10 m $\mu$ .

1	2	3	4	5	1	2	3	4	5
Wavelength	Air mass 0	Air mass 1	Air mass 2	Air mass 3	Wavelength	Air mass 0	Air mass 1	Air mass 2	Air mass 3
<i>m<math>\mu</math></i>					<i>m<math>\mu</math></i>				
299.5	670	25.1	0.9	0.0	367.1	1438	946	622	409
302.5	741	41.9	2.4	.1	368.6	1369	904	597	395
304	1246	112.7	10.2	.9	371	1396	933	623	416
306	1176	157.4	21.1	2.8	375	1102	749	509	346
309.2	1283	245	46.9	8.9	379.4	1462	1005	692	476
310	1045	225	48.7	10.5	380.7	1370	947	655	453
312	1384	370	98.7	26.4	385	945	658	459	320
314.9	1328	419	132.1	41.7	387.7	1156	813	571	401
315.8	1282	429	142.5	48.1	391.5	1441	1021	724	513
316.5	1116	395	138.8	49.6	394	1046	748	535	383
317.9	1415	540	206	78.6	396.1	1209	873	631	456
318.5	1315	504	193	73.4	397.0	1170	848	615	446
321.1	1466	621	263	111.3	403.3	1968	1461	1084	804
321.7	1372	574	240	100.5	406	1870	1401	1050	786
322.8	1272	549	224	91.2	410	1897	1441	1095	832
323.5	1174	519	229	101.2	416.8	1951	1513	1173	909
325.5	1339	617	284	130.7	421	1891	1488	1171	921
327.5	1642	793	383	185	424	1830	1454	1156	919
328.5	1512	747	369	182	428	1569	1267	1023	826
330.3	1705	870	444	226	432	1789	1452	1179	957
331.5	1486	773	402	209	436	1825	1489	1215	992
332.9	1461	772	408	216	441	2001	1651	1362	1124
333.6	1416	754	402	214	447	2080	1735	1447	1209
335.3	1426	773	419	227	455.7	2103	1764	1479	1241
337	1210	668	369	204	468	1933	1639	1390	1178
340.8	1415	799	451	255	482	1978	1677	1441	1226
341.7	1345	765	435	247	487	1832	1591	1349	1157
343.5	1360	780	448	257	497	1904	1643	1417	1223
345	1126	653	379	220	500	1868	1621	1406	1219
348.6	1211	717	423	251	509	1886	1647	1438	1255
351.5	1256	754	453	272	520	1794	1575	1384	1215
352.6	1170	709	429	260	526	1892	1666	1467	1292
355.1	1304	804	496	306	530	1928	1703	1505	1329
358	931	585	366	231	535	1861	1648	1461	1294
360	1164	740	470	298					
361	1097	703	450	288					
363.8	1196	774	502	325					

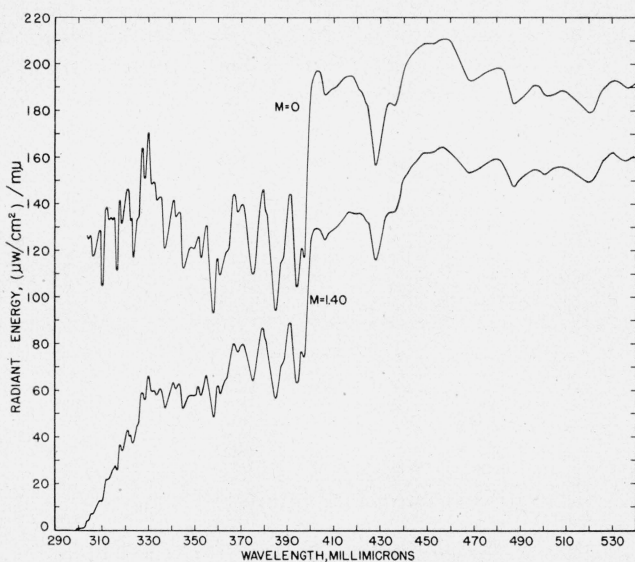


FIGURE 5. Spectral distribution of the radiant energy from the sun.

Climax, Colo., September 1951. (Mean of 4 days.)

Some of the data from table 2 (mean for air mass 1.40 and 0 are shown in figure 5. In order to simplify the illustration of these data, the wavelengths in table 2 for air mass 1.40, were chosen so that they included maxima and minima as well as the points of inflection on the solar energy curve. The data (tables 2 and 3) are nominally tabulated in microwatts per square centimeter per 10 m $\mu$ . They might better be represented in terms of 1-, 2-, or 3-m $\mu$  intervals because the effective slit widths were within this range.

The solar-energy curves shown contain numerous absorption bands varying in magnitude both in spectral width and in intensity of absorption. If reference is made to the Rowland maps and wavelength data [5, 22] and to the Utrecht photometric atlas of the solar spectrum [6], it is found that each band results from one or more groups of intense Fraunhofer lines. In table 4, which lists the approximate wavelengths of the principal absorption bands as recorded in the present investigation, are also listed the principal elements and diatomic molecules responsible for the observed absorption. The wavelength positions of these absorption bands are in close agreement with those of the main concentrations of the winged lines [15] in the solar spectrum.

TABLE 4. Location of principal Fraunhofer absorption regions of the ultraviolet and short-wavelength visible portion of the solar spectrum, and (from the Rowland and Utrecht maps) the elements in the solar atmosphere primarily responsible for the various bands.

Very strong lines result from absorption by the elements marked in boldface type.

Wave-length	Principal absorbing elements
<i>mμ</i>	
310	Fe I, Ni I, Mn I, Al I, OH.
316.5	Fe I, Fe II, Cr II, Ni I, Ti II, OH.
318.5	Ca II, Fe I, Ti I, V II.
323.5	Fe I, Fe II, Ti II, Ni I.
328.5	Fe I, Fe II, Ti I, Ti II, Co I.
331.5	Fe I, Fe II, Zr II, Na I, Ti II, Ni I, Mg I, Co I.
337	NH, Ti II, Ni I, Cr II, Co I.
345	Fe I, Mn II, Ti II, Ni I, Co I.
358	<b>Fe I</b> , Ni I, V II, Sc II, Co I, Ti II, Cr II.
375	<b>Fe I</b> , Ni I, Ti I, Ti II.
385	<b>Fe I</b> , Mg I, CN.
394	Ca II, Al I, H $\epsilon$ .
397	<b>Ca II</b> .
406	H $\delta$ .
428	Fe I.
436	H $\gamma$ .
447	Fe I, Ti I, Ti II, Ca I, Mn I.
468	Mn I, Fe I, Ti II, Ni I.
487	H $\beta$ , Fe I.
500	Fe I, Fe II, Ti I.
520	Mg I.
535	Fe I, Fe II, Ca I, Cr I.

Iron appears to be the principal ultraviolet absorbing material in the solar atmosphere. In spectral regions where some of the other important absorbing materials have superimposed Fraunhofer lines—in particular, the region between about 340 and 397  $m\mu$ , where Ca II, NH, CN, and possibly the Balmer continuum of hydrogen, show strong absorption—there results a spectral region departing significantly from the normal black-body curve. There appears to be little absorption due to Fraunhofer lines and bands near 330  $m\mu$ , and at shorter wavelengths much less than in the 336- to 394- $m\mu$  region, because the envelope of the part of the solar spectrum at wavelengths shorter than 330  $m\mu$  is much closer to that of the expected 6,000° K black-body curve.

#### 4. Atmospheric Transmittance and Ozone

The atmospheric transmission curve, depicted in figure 6 represents the average data for the 4 days (September 16, 17, 19, and 26) covered by tables 2 and 3. In this illustration the logarithm of the observed transmittances of unit atmosphere (at Climax) for the different wavelengths are plotted as a function of the wavelength, which in turn is expanded [21] according to the function  $-(\mu-1)^2\lambda^{-4}$  of the Rayleigh law of molecular scattering,  $\log TR = -32\pi^3(3N)^{-1}(\mu-1)^2\lambda^{-4}H \log e$ . Since for the zenith position the atmospheric depth,  $H$ , and the molecular density,  $N$ ,

are constant, the resulting plot of the logarithm of the atmospheric transmittances becomes a straight line in those spectral regions wherein the Rayleigh law of pure molecular scattering is applicable. In the present case, any scattering, other than molecular was small and simply has been combined with the molecular scattering in giving a straight line of possibly slightly lesser ordinates. At wavelengths shorter than about 340  $m\mu$  ozone absorption enters the picture. This results in transmission data that drop below the straight line representative of scattering alone. The difference in ordinates for any wavelength in this region between the straight line and the observed data is a measure of the ozone absorption for that particular wave length.

In order to translate optical absorption data in the ultraviolet spectral region into specific amounts of ozone, absorption coefficients of the pure gas are required. In the present case, data given by Fabry and Buisson [16] were employed in the calculations of the two curves (fig. 6) representing amounts of ozone required for a similar amount of optical absorption. On the basis of these data, about 0.21 cm of ozone (*ntp*) was present at the time this solar investigation was in progress (September 1951). This value is in close agreement with the average for the same season of the year as obtained for a similar latitude, Washington, D. C. [17].

The multiplicity of Fraunhofer absorption bands (as observed with a prism instrument) in the ultraviolet solar spectrum suggests the need of great care in using a double-prism instrument such as an ozone meter, unless a reasonable region of the spectrum is scanned to assure that intensity settings are being made on specific wavelengths. A very small change, or error, in wavelength calibration may result in the shift of the spectrum setting from a Fraunhofer minimum to a maximum, or vice versa, between two absorption regions. On the other hand, a scanned spectrum, such as that obtained in the present work, offers an ideal method for evaluating ozone, because a definite pair of wavelengths may be chosen with a definite assurance that no error in wavelength setting can be made.

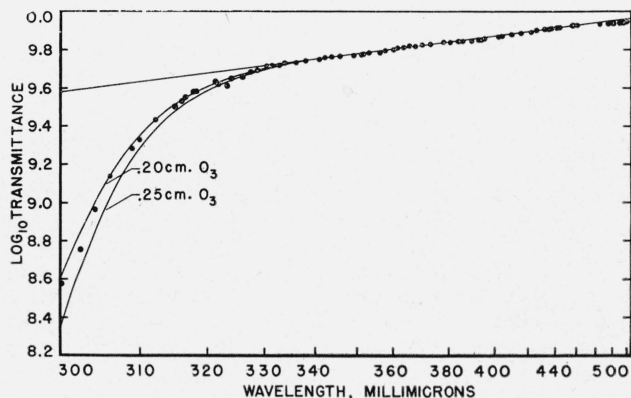


FIGURE 6. Atmospheric transmittance at Climax, Colo., altitude, 11,190 feet; also determination of the total ozone above the observing station.

Upper curve, scattering; lower curves, ozone; ●, atmospheric transmission; mass 1.0, Climax, Colo.; wavelength scale as function of  $-(\mu-1)^2\lambda^{-4}$ .

## 5. Summary and Conclusions

This work, although performed under the expected difficulties of transporting about 1,200 lb of delicate electronic and optical equipment to a more or less isolated mountain station and setting it up and operating it in a temporary building, demonstrates the relative ease with which the ultraviolet spectral distribution of the radiant energy from the sun may be measured with this equipment. From the data obtained, the spectral distribution of the ultraviolet (also part of the visible) radiant energy from the sun has been determined for various air masses at the earth's surface (altitude 11,190 ft) and for outside the earth's atmosphere. From the changes in spectral intensity as a function of air mass (solar angle) the atmospheric transmission coefficients and the total atmospheric ozone content have been determined. These determinations are in good agreement with the best published values. The spectral-energy distribution curve shows much greater Fraunhofer structure than previously reported data for prism instruments. The rapidity of recording assures a complete spectrum before marked changes can occur in intensity as the result of air-mass change.

The relative ease with which the ultraviolet spectral distribution of the radiant energy from the sun may be measured suggests the use of this type of instrument and method for routine use in weather and ozone studies and in the determination of the radiant-energy spectra of some of the brighter stars [23]. Photoelectric equipment of this type is at least a thousand times as sensitive as the best radiometric apparatus presently available. As limited amounts of spectral data have been obtained radiometrically for some of the brighter stars, there appears to be no question regarding the feasibility of using a photoelectric spectroradiometer in conjunction with a large telescope on some of the stars or possibly brighter nebulas.

The author expresses his deep appreciation and gratitude to Walter O. Roberts and other members of the High Altitude Observatory staff for placing the facilities of the Climax station at our disposal and otherwise rendering assistance to us while there; to Norton Baron for helpful assistance in the operation of the equipment in the field; to Russell Johnston for carrying out many of the tedious calculations involved; and to the personnel of the Optics Division of the Naval Research Laboratory for their intense interest and other cooperation in the investigation.

## 6. References

- [1] Ralph Stair, Ultraviolet spectral distribution of radiant energy from the sun, *J. Research NBS* **46**, 353 (1951) RP2206.
- [2] Ralph Stair, Photoelectric spectroradiometry and its application to the measurement of fluorescent lamps, *J. Research NBS* **46**, 437 (1951) RP2212.
- [3] H. A. Bethe, Energy production in stars, *Phys. Rev.* **55**, 434 (1939).
- [4] Ch. Fabry and H. Buisson, L'absorption de l'ultra-violet par l'ozone et la limite du spectre solaire, *J. Phys. Radium* (5) **3**, 196 (1913).

- A. Fowler and R. J. Strutt, Absorption bands of atmospheric ozone in the spectra of sun and stars, *Proc. Roy. Soc. (London)* [A] **93**, 577 (1917).
- Ch. Fabry and H. Buisson, Étude de l'extrémité ultraviolette solaire, *J. Phys. Radium* (6) **2**, 197 (1921).
- Charles Fabry and H. Buisson, A study of the ultraviolet end of the solar spectrum, *Astrophys. J.* **54**, 297 (1921).
- H. Buisson and Ch. Fabry, Mesures de longueurs d'onde dans l'extrémité ultra-violette du spectre solaire, *J. Phys. Radium* (6) **2**, 297 (1921).
- [5] Rowland's map of the solar spectrum. For Rowland's wavelengths, see *Astrophys. J.* **1**, **2**, **3**, **4**, **5** (1895-97). For revised wavelengths, see Revision of preliminary table of solar spectrum wavelengths, etc., by Charles E. St. John, et al., Carnegie publication No. 396 (1928).
- [6] M. Minnaert, G. F. W. Mulders, and J. Houtgast, The Utrecht photometric atlas of the solar spectrum (*J. Schnabel*, Amsterdam 1940).
- [7] R. Stair and W. O. Smith, A tungsten-in-quartz lamp and its applications in photoelectric radiometry, *J. Research NBS* **30**, 449 (1943) RP1543.
- [8] Deane B. Judd, The 1949 scale of color temperature, *J. Research NBS* **44**, 1 (1950) RP2053.
- [9] W. E. Forsythe and A. G. Worthing, The properties of tungsten and the characteristics of tungsten lamps, *Astrophys. J.* **61**, 146 (1925).
- [10] F. Hoffman and H. Willenberg, Das Emissionsvermögen des Wolframs in ultraviolet bei hohen Temperature, *Physik. Z.* **35**, 1, 711 (1934).
- [11] H. C. Hamaker, Reflectivity and emissivity of tungsten, Inaug. Diss. (Utrecht, Holland, 1934).
- [12] L. S. Ornstein, Tables of the emissivity of tungsten as a function of wavelength from 0.23 to 2.0  $\mu$  in the region of temperature 1600° to 3000° K, *Physica* **3**, 561 (1936).
- [13] H. T. Wensel, D. B. Judd, and W. F. Roeser, Establishment of a scale of color temperature, *BS J. Research* **12**, 527 (1934) RP677.
- [14] Deane B. Judd, The 1931 I. C. I. standard observer and coordinate system for colorimetry, *J. Opt. Soc. Am.* **23**, 360 (1933).
- [15] Charlotte E. Moore and Henry Norris Russell, On the winged lines in the solar spectrum, *Astrophys. J.* **63**, (1926).
- [16] C. Fabry and H. Buisson, Data on ozone absorption, *Compt. rend.* **192**, 457 (1931).
- [17] Ralph Stair, Seasonal variation of ozone at Washington, D. C., *J. Research NBS* **43**, 209 (1949) RP2022.
- [18] Helen W. Dodson, Solar flares, *Astrophys. J.* **110**, 382 (1949).
- [19] Helen W. Dodson and E. Ruth Hedeman, The frequency and positions of flares within three active sunspot areas, *Astrophys. J.* **110**, 242 (1949).
- [20] Helen W. Dodson and Robert W. Donselman, The eruptive prominence of August 7, 1950, *Astrophys. J.* **113**, 519 (1925).
- [21] Edison Pettit, Spectral energy-curve of the sun in the ultraviolet, *Astrophys. J.* **91**, 159 (1940).
- [22] Harold D. Babcock, Charlotte E. Moore, and Mary F. Coffeen, The ultraviolet solar spectrum, 2935-3060A, *Astrophys. J.* **107**, 287 (1948).
- [23] C. G. Abbot and L. B. Aldrich, Energy spectra of some of the brighter stars, *Smithsonian Misc. Collections* **107**, No. 19 (Pub. No. 3914, 1948).
- [24] Joel Stebbins and A. E. Whitford, Six-color photometry of stars. The colors of extragalactic nebulae, *Astrophys. J.* **108**, 413 (1948).
- [25] F. W. Paul Götz and Ernst Schönmann, Die spektrale Energieverteilung von Himmels- und Sonnenstrahlung, *Helv. Phys. Acta* **21**, 151 (1948).
- [26] Heinz Reiner, Die Struktur des Sonnen Spectrums Zwischen 400 und 600 m $\mu$ , *Garlands Beitr. Geophys.*, **55**, Heft 2, 234 (1939).

WASHINGTON, May 5, 1952.